Regional Studies in Marine Science 24 (2018) 55–65

Contents lists available at ScienceDirect

Regional Studies in Marine Science

journal homepage: www.elsevier.com/locate/rsma

Physical forces determine the annual bloom intensity of the giant jellyfish *Nemopilema nomurai* off the coast of Korea

Jang-Geun Choi [a], Young-Heon Jo [a,*], Il-Ju Moon [b], Jinku Park [a], Dae-Won Kim [a], Thomas C. Lippmann [c]

[a] *Department of Oceanography, Pusan National University, Busan, 609-735, Republic of Korea*
[b] *College of Ocean Science, Jeju National University, Jeju, 690-756, Republic of Korea*
[c] *Department of Earth Sciences, Center for Coastal and Ocean Mapping, University of New Hampshire, Durham, NH, United States*

ARTICLE INFO

Article history:
Received 8 September 2017
Received in revised form 3 July 2018
Accepted 10 July 2018

ABSTRACT

During the summer, giant jellyfish (*Nemopilema nomurai*) are transported from their main seeding and nursery ground, Jiangsu Province and the coast of China, to Korean coastal waters by the currents of the Yellow Sea (YS) and the East China Sea, causing problems for swimmers and hampering fisheries. In this study, we derive new velocity fields based on satellite measurements and develop particle-tracking experiments to simulate and analyze the interannual change of *N. nomurai* abundance off the coast of Korea. The velocity fields are calculated by combining Ekman currents and geostrophic currents based on an analytical solution of an approximated momentum equation. For validation, we compare the particle-tracking experiment results with *in situ* observations obtained from the Korean National Institute of Fisheries Science. The combined velocity fields during the summer show that geostrophic currents are of the same order as Ekman currents over the YS, implying that the interannual changes in *N. nomurai* abundance off the coast of Korea are determined by combined Ekman and geostrophic currents. In addition, *N. nomurai* distribution off the coast of China in April is considered an important factor driving blooms around Korean coasts. To test this supposition, we conducted a sensitivity experiment that adjusted the position of particles off the coast of China in April. Results demonstrate that the appearance of *N. nomurai* can increase by a factor of three depending on the initial distribution of the jellyfish off the coast of China before eastward transport in April.

1. Introduction

Nemopilema nomurai is a giant jellyfish, with origins generally considered to be the Jiangsu Province and the coast of China (Yoon et al., 2008; Moon et al., 2010; Toyokawa et al., 2012; Wei et al., 2015; Sun et al., 2015). Fig. 1 shows a schematic diagram of the *N. nomurai* life cycle (Kawahara et al., 2006; Uye, 2008). During early summer, benthic polyps start strobilation and generate pelagic ephyra stages. Young *N. nomurai* mature and become medusa. *N. nomurai* is transported to the east during the summer by ocean currents in the Yellow Sea (YS) and East China Sea (ECS) and begin to appear off the coast of Korea. The appearance of *N. nomurai* off the coast of Korea causes enormous damage to the ocean environment and associated industries by decreasing fisheries catch and injuring caught fishes (Kim et al., 2012; Yoon et al., 2014). As a result, observations of *N. nomurai* have been obtained by the Korean National Institute of Fisheries Science (NIFS) since 2006. In particular, the appearance of *N. nomurai* in the YS and ECS has been surveyed using research vessels and small airplanes.

Yoon et al. (2014) reported that the appearance of *N. nomurai* has become an annual event around the coast of the Korean Peninsula since 2002. According to their observations, *N. nomurai* are sighted in the northwest ECS and move toward the southeast YS in May. From July to October, *N. nomurai* appear in all seas off the Korean coast. After October, they retreat westward from the Korean coast, following the regional current system and slowly disappear from the Korean Peninsula. Observations show high correlation between the dispersion of Changjiang diluted water and the appearance of *N. nomurai*, which suggests that the *N. nomurai* population moves with the Changjiang diluted water, reaching the coast of Jeju Island and even the East/Japan Sea (Yoon et al., 2008, 2012).

Geographic locations and current systems of the YS and ECS are illustrated in Fig. 2. The YS is surrounded by mainland China and the Korean Peninsula and is connected to the ECS; it has an average depth of 44 m. The YS has a complex current system which can be influenced by both tidal and subtidal components

* Corresponding author.
E-mail address: joyoung@pusan.ac.kr (Y.-H. Jo).

https://doi.org/10.1016/j.rsma.2018.07.003
2352-4855/

(Kim, 1998). Intrusion of the Kuroshio Current branch and wind stress from the East Asian Monsoon can govern the seasonal current pattern of the YS (Naimie et al., 2001; Hsueh et al., 1986). The East Asian Monsoon system generally produces northerly winds during the winter and southerly winds during the summer. As a result, southwestward and northeastward Ekman surface currents occur during winter and summer, respectively. During the summer, the southerly winds are relatively weak and less consistence, thus forcing from oceanic low-pressure systems induced by a dense and low-temperature water mass (known as Yellow Sea Cold Water, Fig. 2) becomes more dominant in the YS (Naimie et al., 2001). This indicates that seasonal current systems of the YS are controlled by pressure gradients and wind stress (Mask et al., 1998; Park, 1986).

Various studies based on numerical models have simulated the transport of *N. nomurai*. Moon et al. (2010) simulated *N. nomurai* transport in 2005 from May to July in the YS and ECS using a particle-tracking model within the Regional Ocean Modeling System (ROMS; Song and Haidvogel, 1994). To drive the model, they used various types of atmospheric and oceanic forcing, such as wind stress, freshwater flux, heat flux, river discharge, and changes in the lateral boundary conditions of ocean temperature, salinity, and velocity. The study concluded that wind stress plays an important role and Ekman currents determine the distribution of *N. nomurai*.

Japan's Fisheries Research Agency also developed a particle-tracking approach for considering the vertical migration of *N. nomurai* based on the Japan Sea Data Assimilation Experiment (Okuno et al., 2011). Using a particle-tracking approach, they modeled *N. nomurai* transport in the East/Japan Sea in September 2009. Later, they considered temperature as a key parameter in the vertical migration and mortality of *N. nomurai*, and thus successfully simulated a more realistic vertical distribution of *N. nomurai* in the East/Japan Sea in 2009.

Wei et al. (2015) also used particle-tracking experiments to simulate *N. nomurai* behavior off the east coast of China from May to September in 2008 and 2009. They applied tidal forcing to a numerical model and considered ecological perspectives such as vertical migration and the conditions required for the birth of *N. nomurai*, which is triggered by temperature. The study concluded that physical circulation is more important than biological supplementation for understanding the horizontal distribution of *N. nomurai* off the coast of China and in the YS.

Most of the previous studies have focused only on events over the short time periods of *N. nomurai* appearances using numerical models. In contrast, we propose to use diagnostic velocity fields based on satellite remote sensing measurements. Yanagi et al. (1997) calculated the seasonal mean geostrophic current fields of the YS and ECS from satellite altimetry and verified the velocity fields using a numerical model and buoy measurements. Velocity fields in this study are obtained by combining geostrophic current data with wind stress data using the analytical solution of the approximated momentum equation from Welander (1957). In addition, we highlight the simulation of interannual *N. nomurai* appearance changes off the coast of Korea using the combined velocity fields based on satellite measurements and particle-tracking experiments. By analyzing simulation results and velocity fields, physical factors that determine the amount of *N. nomurai* transported toward the Korean Peninsula are discussed.

In Section 2, the velocity fields and particle tracking experiments are considered together with observations in the study area. In Section 3, we simulated the transport of *N. nomurai* observed by NIFS using particle-tracking experiments to validate the velocity fields. We then conduct simulations of the long-term and inter-

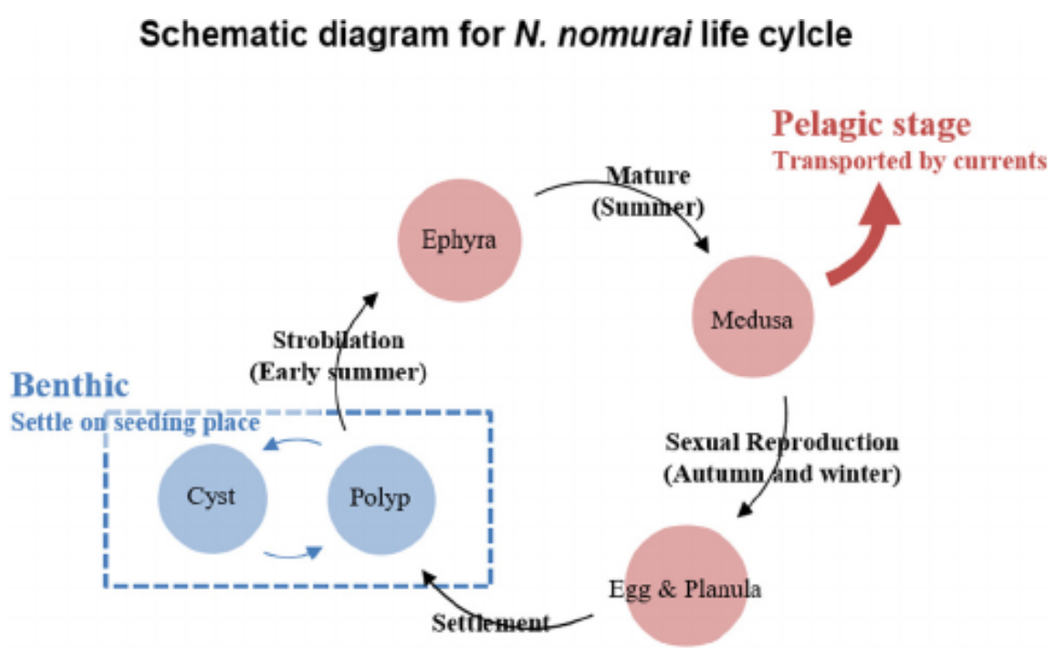

Fig. 1. Schematic diagram of *N. nomurai* life cycle. Blue and red circles indicate benthic and pelagic life stages, respectively. (For interpretation of the references to color in this figure legend, the reader is referred to the web version of this article.)

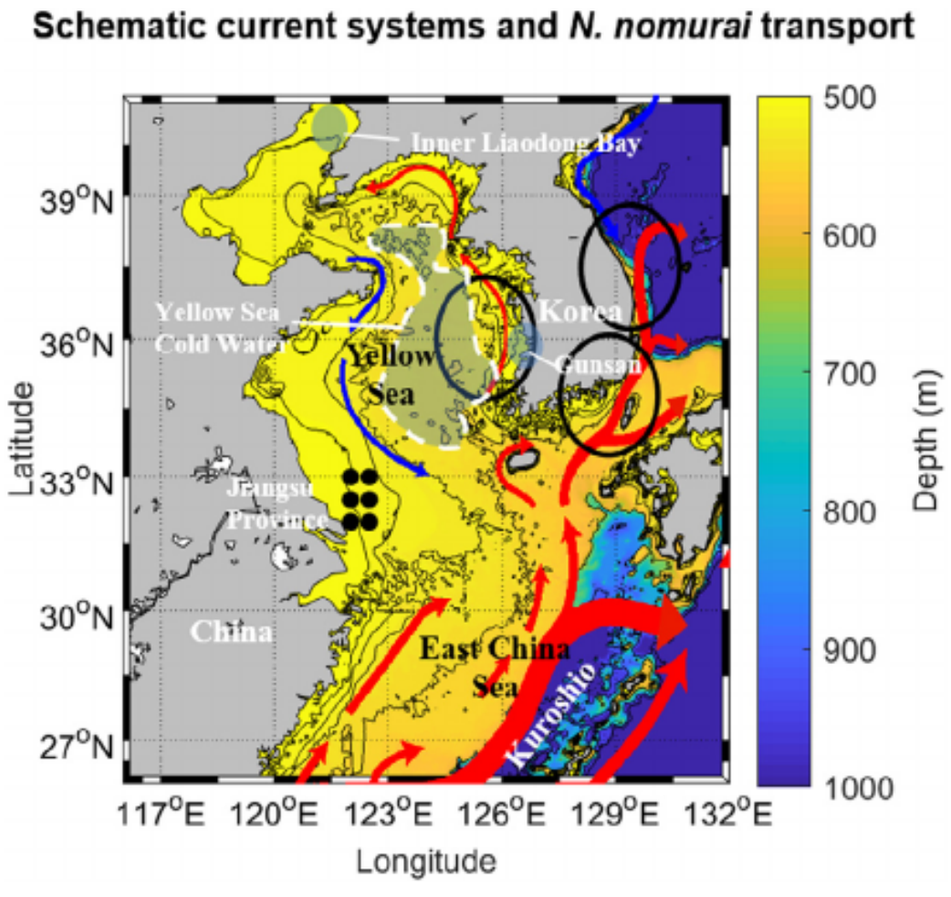

Fig. 2. Geographical location and current systems of the YS and ECS. Black dots are the initial positions of the particle-tracking experiment in Section 3.2. The circles are for counting particles that appeared off the coast of Korea. Red and blue arrows indicate warm and cold currents in the study area, respectively. (For interpretation of the references to color in this figure legend, the reader is referred to the web version of this article.)

2. Data and methods

For ocean current data we use absolute geostrophic velocities derived from satellite altimetry measurements. These measurements were obtained through Archiving, Validation and Interpretation of Satellite Oceanographic data (AVISO) (available at http://www.aviso.altimetry.fr/en/data/products). Its spatial and temporal resolution is 0.25° × 0.25° and 1 day, respectively. Although there are intrinsic measurement inaccuracies (particularly in coastal areas) due to wet troposphere, sea surface height bias, orbit determination, and other factors (Ablain et al., 2009), such data can be used for seasonal circulation patterns in the YS and ECS (Yanagi et al., 1997).

We calculate wind stresses using ERA-Interim reanalysis data. This reanalysis dataset is provided by the European Centre for Medium-Range Weather Forecasts (available at http://www.ecmwf.int/en/research/climate-reanalysis), which has been tested

annual changes in *N. nomurai* appearances off the coast of Korea from 2006 to 2015. In Section 4, the results are discussed and summarized.

to ensure stable data assimilation systems and provides various atmospheric data (Dee et al., 2011). The spatial and temporal resolution is 0.25° × 0.25° and 6 h, respectively. For bathymetry,

we used ETOPO1 data, which are composed of numerous datasets from the U.S. National Oceanic and Atmospheric Administration (NOAA; Amante and Eakins, 2009). The spatial resolution is 1 arcmin. The data with different spatial and temporal resolution were interpolated to 0.25° × 0.25° and 6 h intervals to coincide with velocity fields. In addition, *in situ* distribution of *N. nomurai* appearances were obtained from NIFS (available at http://www.nifs.go.kr/bbs?id=jellynews) to verify the results of this study. The *N. nomurai* appearances were recorded by fishermen and reported as a proportion of fishermen observing jellyfish for a given week among the entire fishing fleet.

2.1. Sea surface currents from geostrophic and Ekman currents

Velocity fields that combine wind stress and geostrophic currents are calculated based on an approximated momentum equation that considers three terms representing vertical eddy mixing, pressure gradients, and Coriolis. Similar approaches have been used and verified in previous studies calculating sea surface current fields based on altimetry measurements. Saraceno et al. (2008) showed that geostrophic current fields become more comparable with *in situ* surface currents by simply adding the analytical solution for Ekman flow assuming infinite water depth and constant Ekman depth. Bonjean and Lagerloef (2002) also used the same momentum with an additional buoyant term representing the thermal-wind contribution. Their methodology was used as the basis for OSCAR (Ocean Surface Current Analysis Real-time) surface velocity fields provided by NOAA (https://podaac.jpl.nasa.gov/dataset/OSCAR_L4_OC_third-deg). Johnson et al. (2007) showed that the OSCAR surface velocity fields have more comparable probability distribution with observations than data-assimilated numerical models, and suggested that the former velocity fields could be better than the latter to simulate object-tracking and tracer dispersion experiments. However, because OSCAR velocity fields are optimized for large scale and vertically integrated, they represent averaged sea surface currents above 30 m (Johnson et al., 2007). Therefore, OSCAR velocity fields were deemed inappropriate for simulating surface drifting objects in marginal shallow water such as the YS.

In this study, surface current velocity fields are obtained by calculating the exact solution to the balance between the vertical eddy mixing, pressure gradient, and Coriolis force (Welander, 1957). The governing equations and boundary conditions are given by

$$\begin{aligned} \vec{u} &= \vec{u}_e + \vec{u}_g \\ f\vec{\mathrm{k}} \times \vec{u} &= -\frac{\nabla \mathrm{P}}{\rho} + A_z \frac{\partial^2 \vec{u}}{\partial z^2} \\ \rho A_z \frac{\partial \vec{u}_e}{\partial z} &= \vec{\tau} \qquad @\, z = 0 \\ \vec{u} &= 0 \qquad @\, z = -\mathrm{h} \end{aligned} \tag{1}$$

where $\vec{u}$ is the horizontal velocity in the Cartesian coordinate system and has two complex components representing the Ekman ($\vec{u}_e$) and geostrophic ($\vec{u}_g$), $\vec{u}_e = u_e + iv_e$ is the zonal (u_e) and meridional (v_e) Ekman component, $\vec{u}_g = u_g + iv_g$ is the zonal (u_g) and meridional (v_g) geostrophic component, $\vec{\tau} = \tau_x + i\tau_y$ is the zonal (τ_x) and meridional (τ_y) wind stress, ρ is the density of seawater, A_z is the vertical eddy viscosity coefficient, h is depth, and z is the vertical coordinate. The analytical solution of Eq. (1) is given by

et al., 2017). In addition, contributions of geostrophic components for the total combined velocity were defined as

$$\frac{\vec{u}_g}{\vec{u}_e + \vec{u}_g} \times 100. \tag{3}$$

For *N. nomurai* transport, Eq. (3) is used to estimate the relative importance of Ekman and geostrophic components.

2.2. Particle tracking scheme and random walk

To conduct the particle-tracking experiments, we use a fourth-order Runge–Kutta scheme to prevent excessively large truncation errors. Random walk was also considered to resolve sub-grid scale phenomenon, such as horizontal turbulent flow and swimming of the individuals (Willis, 2011). This term is defined as $\mathrm{N}\sqrt{2\mathrm{K_h}\Delta \mathrm{t}}$, where N is a normally distributed random number, Δt is time step of the particle-tracking experiment, and $\mathrm{K_h}$ is the horizontal diffusivity coefficient based on the Smagorinsky diffusivity scheme,

$$\mathrm{K_h} = \mathrm{A}\,\Delta \mathrm{x}\Delta \mathrm{y}\sqrt{\left(\frac{\partial \mathrm{u}}{\partial \mathrm{x}} - \frac{\partial \mathrm{v}}{\partial \mathrm{y}}\right)^2 + \left(\frac{\partial \mathrm{v}}{\partial \mathrm{x}} + \frac{\partial \mathrm{u}}{\partial \mathrm{y}}\right)^2}. \tag{4}$$

where Δx and Δy are the grid spacing, and A is an adjustment constant defined as 0.02 (Sheng et al., 2009; Okuno et al., 2011). In essence, *N. nomurai* is considered passive particles without biological behavior (except within the random walk parameterization).

2.2.1. N. nomurai population tracking experiment

To clarify the performance of the velocity fields for surface particle tracking experiments, we simulated transport of *N. nomurai* populations that were observed, predicted the distribution of the jellyfish over time, and compared results with the observed *in situ* distributions. Two *N. nomurai* groups were observed by NIFS at 124°E, 32°N and 125°E, 32° N on May 26, 2012 (Fig. 3a) and observed again southwest of Jeju Island on July 12 (Fig. 3b). Based on this observation, 10,000 and 5000 particles, respectively, were released at the two positions within the velocity fields at the time when the jellyfish groups were first observed. Simulation results are discussed in Section 3.2.

2.2.2. Simulation of interannual N. nomurai appearances off the coast of Korea

We conducted particle-tracking experiments to simulate *N. nomurai* appearances off the coast of Korea from 2006 to 2015. Five particles per day were deployed from March to November at six initial points (Fig. 2, black dots) off the coast of Jiangsu Province. Even though there are two additional possible seeding places –the inner part of Liaodong Bay and Gunsan (Fig. 2, Sun et al., 2015) – Jiangsu Province is generally considered to be the primary seeding location of *N. nomurai* (Yoon et al., 2008; Moon et al., 2010). We counted the number of particles in three areas (Fig. 2, circles), and compared with observed *N. nomurai* appearances (Section 3.3).

2.2.3. Comparison with velocity fields from HYCOM reanalysis data

We compared the surface current patterns in the YS and ECS from the combined velocity fields with those from the Hybrid Coordinate Ocean Model (HYCOM) reanalysis data, which have been used previously to address complex ocean dynamics near the Korean Peninsula (Seo et al., 2013; Hong et al., 2016). To compare

$$\vec{u}_e = \frac{\vec{\tau}}{\rho A_z j}\frac{\sinh[j(h+z)]}{\cosh(jh)} - \frac{\cosh(jz)}{\cosh(jh)}\vec{u}_g \quad (2)$$

where $j = (1+i)\sqrt{f/2A_z}$. Because most jellyfish float on the sea surface (Honda et al., 2009), sea surface velocities were used at $z = 0$, and $A_z = 10^{-3}$ m^2/s was assumed to be constant (Zhang

the relative performance of hindcasts of surface particle transport in the YS and ECS, the particle tracking experiments mentioned in Sections 2.2.1 and 2.2.2 were reproduced using the HYCOM velocity fields. Identical initial conditions were used for both simulations; only the velocity fields from the combined velocity fields were replaced to those of HYCOM.

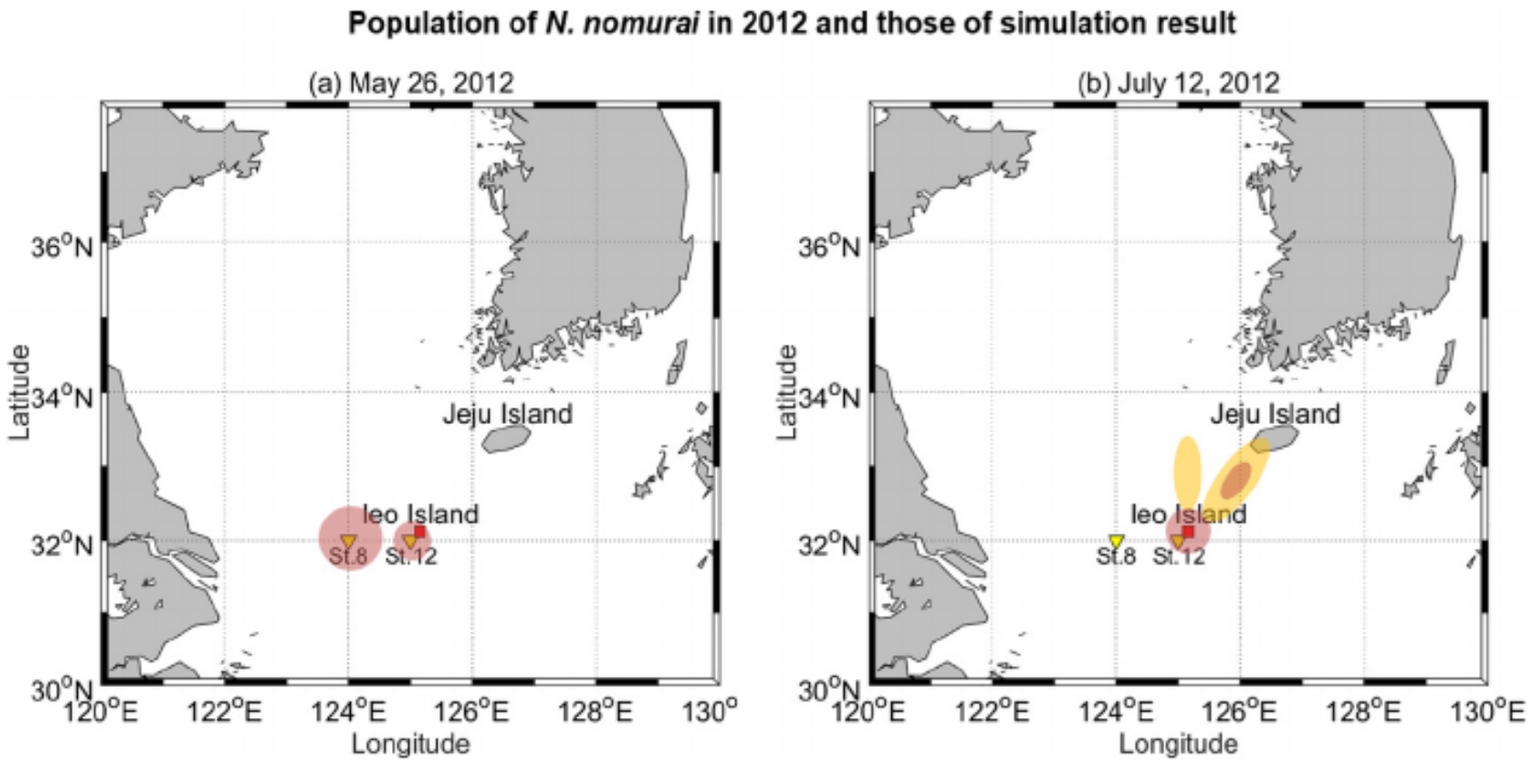

Fig. 3. (a) *N. nomurai* distribution in the YS and ECS observed by NIFS in May 2012, (b) observed jellyfish group in July. In (a) and (b), red and yellow areas indicate high and low density of *N. nomurai* individuals, respectively. (For interpretation of the references to color in this figure legend, the reader is referred to the web version of this article.) *Source:* (a) and (b) were adapted images from NIFS (available at http://www.nifs.go.kr/bbs?id=jellynews).

3. Results

3.1. Combined velocity fields for particle-tracking experiments

The combined velocity fields resolve the seasonal surface current patterns of the YS and ECS. Fig. 4 shows summer (June–August) and winter (December–February) mean Ekman current fields (Fig. 4a and b), geostrophic current fields (Fig. 4c and d), and the combined surface current fields and contributions of geostrophic currents (Fig. 4e and f). During winter, the combined velocity fields reflect strong southeastward currents that are mainly driven by wind stresses (Fig. 4f). However, during the summer Ekman currents become relatively weaker than during winter, and the contribution of geostrophic currents increases (Fig. 4e). This pattern coincides with the intensification of low-pressure systems driven by Yellow Sea Cold Water (Mask et al., 1998; Park, 1986; Naimie et al., 2001). The velocity fields show surface currents matching the reported surface circulation patterns in the YS and ECS. For instance, a clockwise current off the south coast of China to Jeju Island was observed in July and an oppositely directed current developed from September to October. In addition, the northeastward current off the south coast of China in July changes its direction to southwestward in October, which also agrees with observations (Moon et al., 2010; Ichikawa and Beardsley, 2002).

Fig. 5 shows summer and winter mean climatological velocity fields obtained by HYCOM global reanalysis data from 2006 to 2012. The velocity fields show similar circulation patterns as the combined velocity fields used in this study; relatively weak northeastward currents during summer (Fig. 5a) and strong southwestward currents during winter (Fig. 5b). However, there were also differences. In particular, the Yellow Sea Warm Current, a branch of the Kuroshio Current that intrudes into the YS, frequently appeared in the surface HYCOM velocity fields during the summer. This current became more dominant in August, and figures prominently in the monthly mean velocity fields from HYCOM (Fig. 6a). Conversely, the combined velocity fields did not show the Yellow

3.2. N. nomurai population tracking experiment results

We conducted additional tests by tracking observed *N. nomurai* groups using the combined velocity fields and particle-tracking experiments. Fig. 7a shows simulated particles on 12 July 2012 using the combined velocity fields. All particles moved westward from their original location and then bifurcated; most moved southward but some moved northward and entered the YS. By the end of June the paths of all particles deflected eastward in response to wind stress. The distribution of the simulated particles on 12 July 2012, displayed in Fig. 7a, shows a group of highly concentrated particles that appeared between Jeju Island and Ieo Island. This result agrees with NIFS observations of *N. nomurai* distribution also located between Jeju and Ieo Islands in July (Fig. 3b), and suggests that the particle-tracking experiment using the velocity fields derived in this study can be used to reasonably simulate jellyfish advection. For the jellyfish population tracking experiment using HYCOM, simulated particles were transported by the Yellow Sea Warm Current and moved more northwestward than the simulation result using the combined velocity fields. Consequently, particles were located at center of the YS on July (Fig. 7b), which did not correspond to the observed distributions (Fig. 3b).

3.3. Simulation for interannual changes of N. nomurai appearance using particle-tracking experiments

Fig. 8 shows the climatological distribution of particles that represent typical seasonal changes of the jellyfish distribution. In March the particles were concentrated off the east coast of China because of strong southwestward Ekman currents. Starting in April the winds weakened and their direction changed. Some particles moved away from the coast of China, began to move slowly northeastward, and arrived off the coast of the Korean Peninsula in June. After June, the particles continuously moved toward the Korean Peninsula and became concentrated. Some particles were

Sea Warm Current (Fig. 6b). This current is frequently generated by some numerical models, but clear observational evidence has not been found (Beardsley et al., 1992; Teague and Jacobs, 2000; Ichikawa and Beardsley, 2002; Tang et al., 2004). Recent studies and observations show that the Yellow Sea Warm Current sporadically appears during winter (Teague and Jacobs, 2000; Lie et al., 2001). In addition, Yu et al. (2010) suggested that the Yellow Sea Warm Current is stably observed near the bottom of the west part of YS during winter, but not a persistent current in the surface layer.

transported to the Korean Strait and further toward the East/Japan Sea. In September, as southwestward Ekman currents intensified, particles retreated toward the ECS. These seasonal changes in particle distribution correspond to the observed patterns of *N. nomurai* appearances.

Fig. 9 shows comparisons between particles simulated by the particle-tracking experiment and *in situ* measurements of *N. nomurai* appearances. The blue line indicates the total number of particles in the three areas, whereas the red line indicates *N. nomurai* appearances off the coast of Korea as observed on site by NIFS.

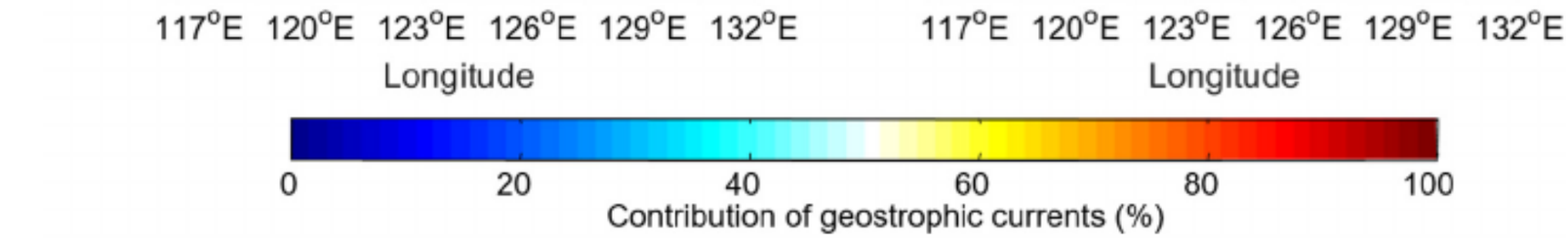

Fig. 4. Summer and winter mean velocity fields of the Ekman current (a) and (b), geostrophic current (c) and (d), and combined flows (e) and (f). Color scale in (e) and (f) indicate contribution of geostrophic currents for the combined velocity fields.

We added red circles to Fig. 9 to show the *N. nomurai* appearances reported by Yoon et al. (2014). The maximum correlation between simulations and observations is 0.77, with a 35-day lag in which the simulated particles lead the data. The 95% significance level (0.41) was determined by bootstrap methods defined in Ebisuzaki (1997). In each year except for 2010 and 2011, particle abundances

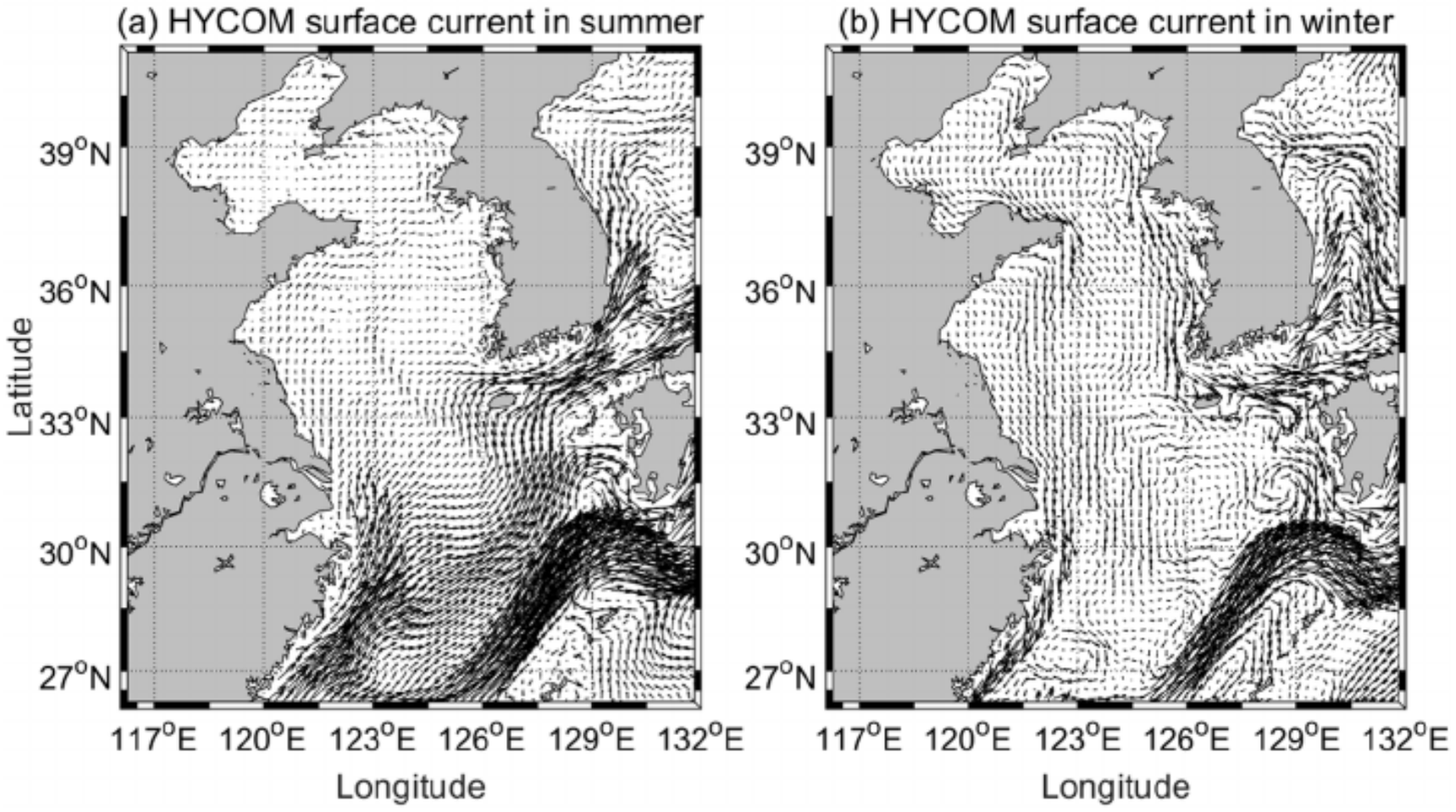

Fig. 5. HYCOM surface velocity fields during summer (a) and winter (b) from 2006 to 2012.

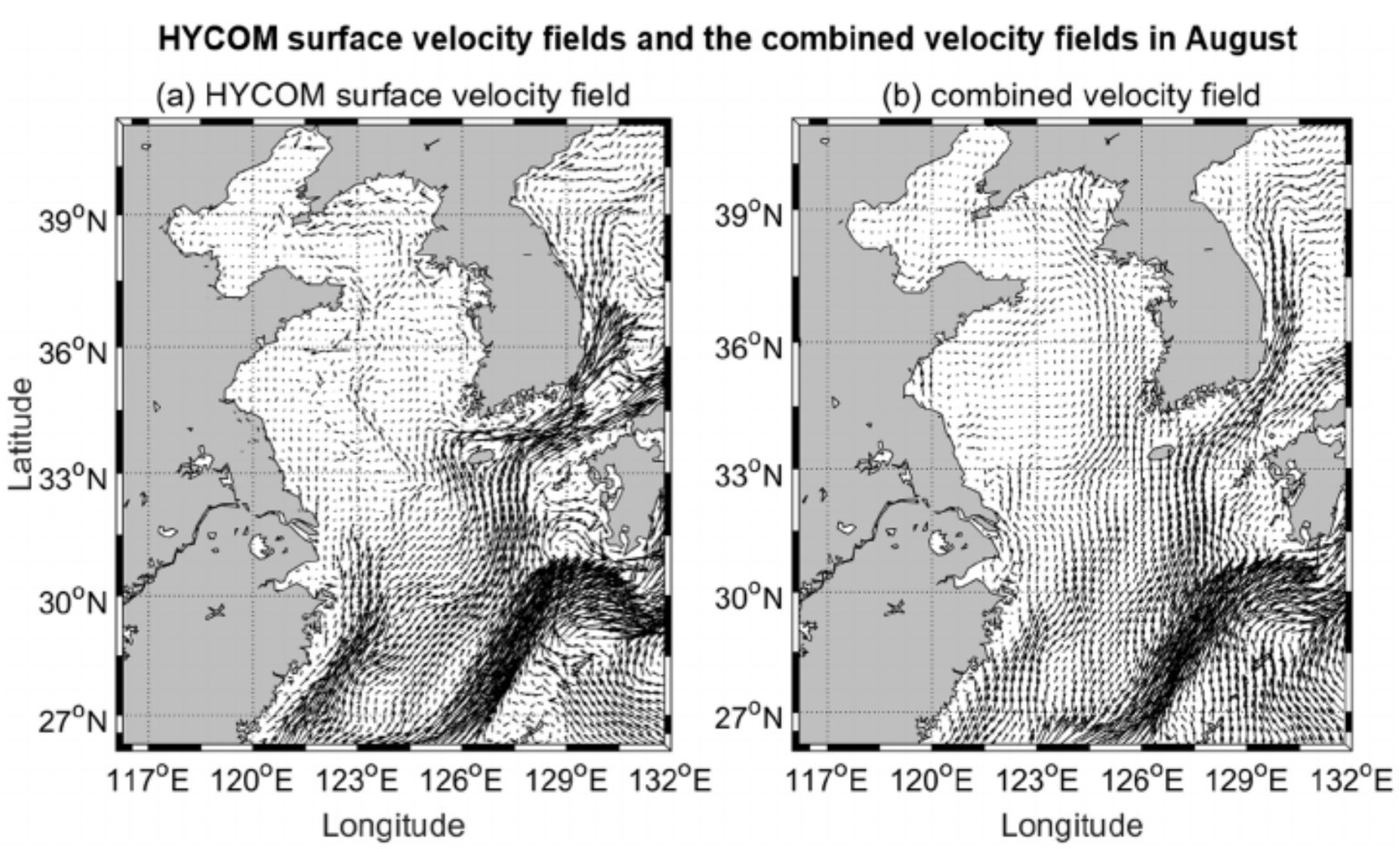

Fig. 6. Climatological mean velocity fields in August from HYCOM reanalysis (a) and the combined velocity fields (b).

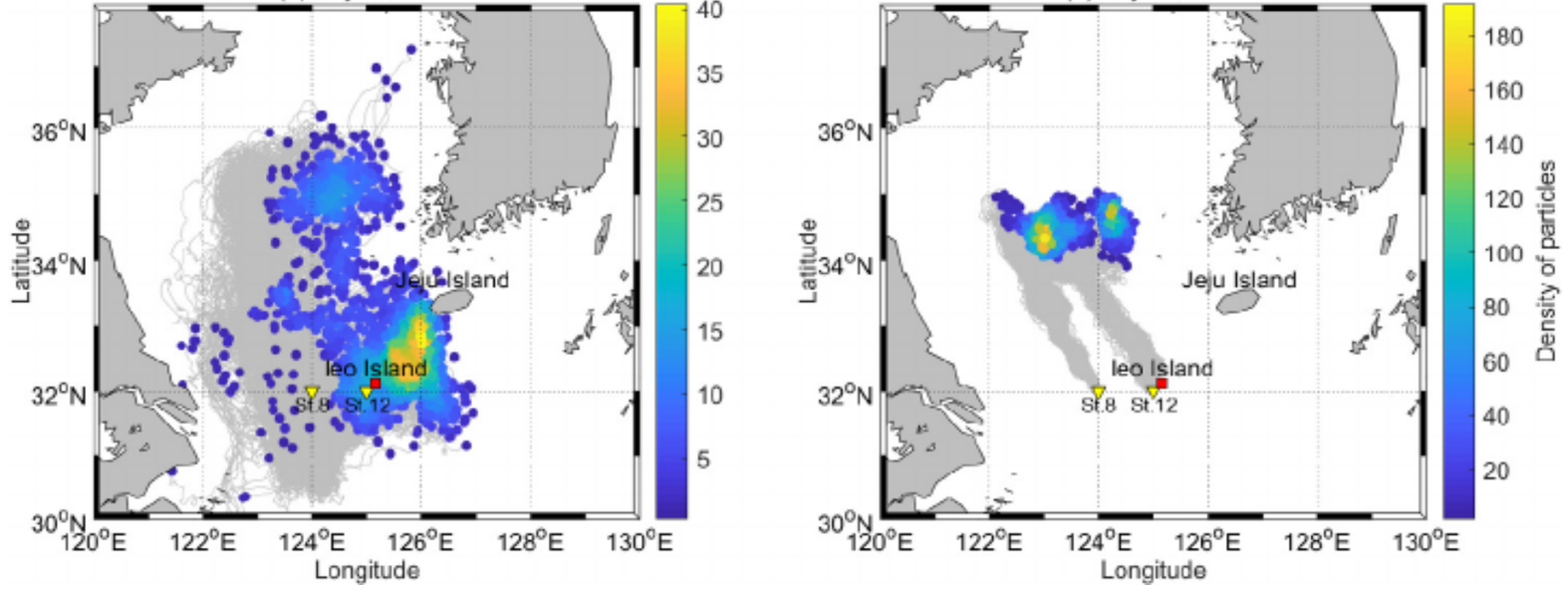

Fig. 7. Population tracking experiment results using the combined velocity fields (a) and HYCOM reanalysis dataset (b). Color scale indicates particle density.

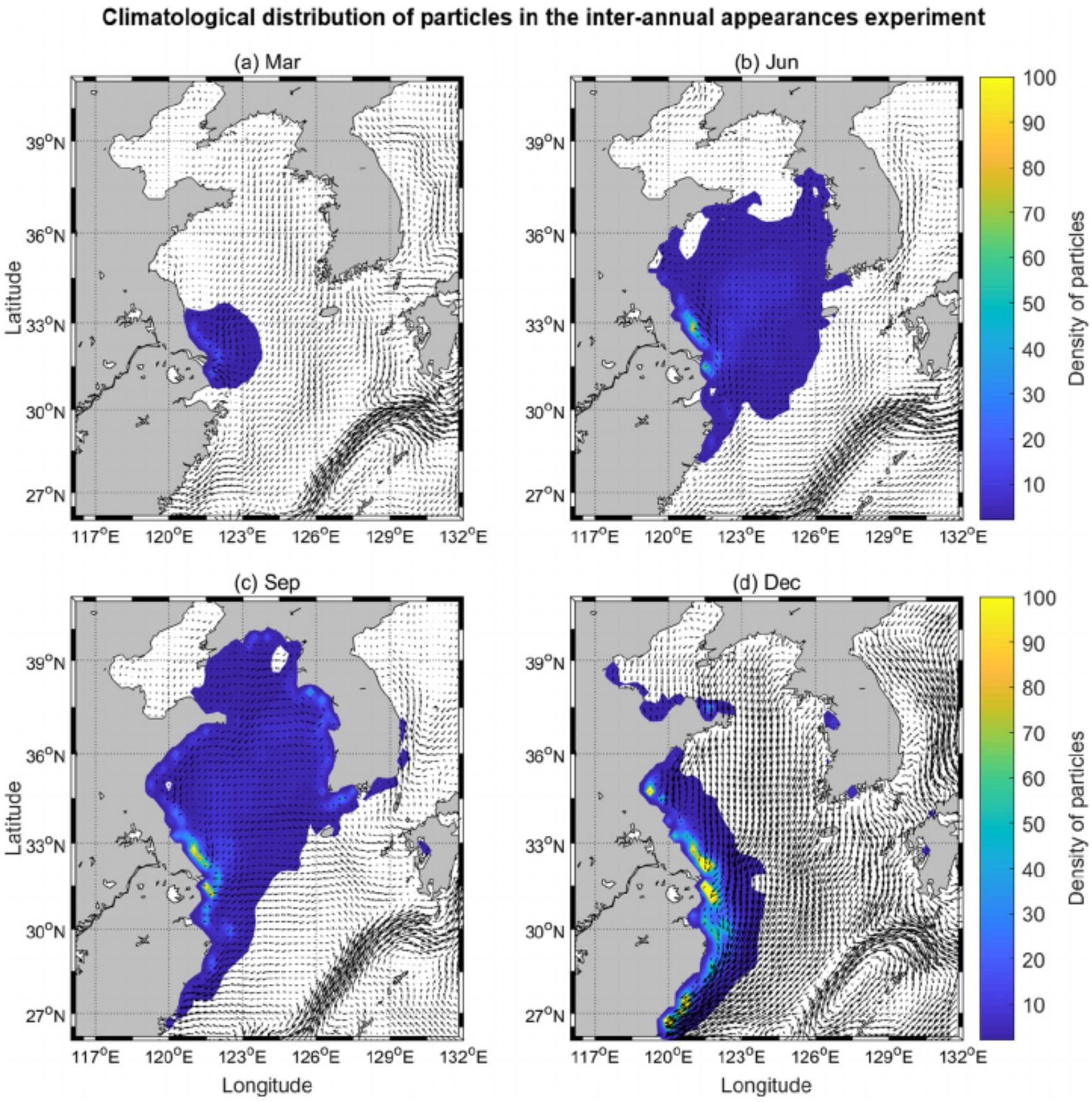

Fig. 8. Results of the particle-tracking experiment from 2006 to 2015, and indicate climatological distribution of particles. Color scale indicates particle density.

generally agree with the observations of maximum *N. nomurai* appearances. Consequently, the combined velocity fields that comprise Ekman and geostrophic currents appear to simulate plausible interannual changes of *N. nomurai* appearances, which implies the importance of the Ekman and geostrophic currents for *N. nomurai* transport. An equivalent simulation was conducted using velocity fields from HYCOM reanalysis data from 2006 to 2012. Although the general pattern of jellyfish appearances is reproduced, the

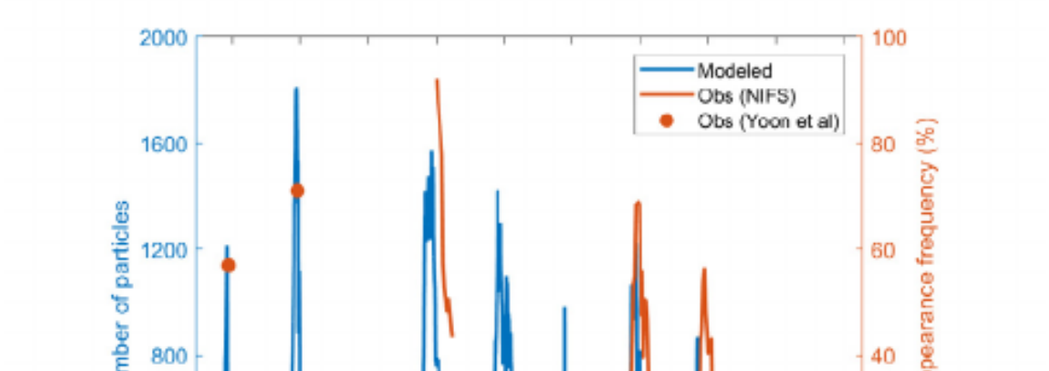

number of particles that arrived at the coast of Korea was less than that predicted using the combined velocity field, and less correlated (0.42 vs. 0.77) with observations (Fig. 10).

4. Discussion and conclusion

4.1. Validation of particle-tracking experiments based on the combined velocity fields

There are certain limitations to the results in this study. For instance, in Fig. 3, the NIFS-observed locations of *N. nomurai* and those of the simulated particles do not precisely match, with discrepancies of approximately 0.5°. Furthermore, simulation of the jellyfish appearances do not provide reasonable results in 2010 and 2011, with simulated particles arriving earlier off the coast of Korea than observed (Fig. 9). These discrepancies may be due to simplifying assumptions in the momentum equation of Welander (1957), or by uncertainties in the nearshore region of the mapped sea surface height data provided by AVISO (Saraceno et al., 2008). This issue also contributes to incorrect alongshore coastal current

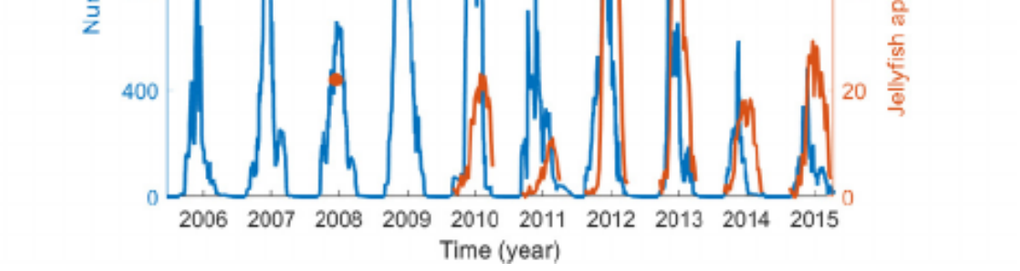

Fig. 9. Comparison between simulated particles using combined velocity fields and the appearances of *N. nomurai* off the coast of Korea. The blue line indicates the total number of particles in the coastal area of the Korean Peninsula (Fig. 1, circles). The red line indicates the appearances of *N. nomurai* off the coast of Korea as reported by NIFS. Red circles show the appearances of *N. nomurai* as reported by Yoon et al. (2014). (For interpretation of the references to color in this figure legend, the reader is referred to the web version of this article.)

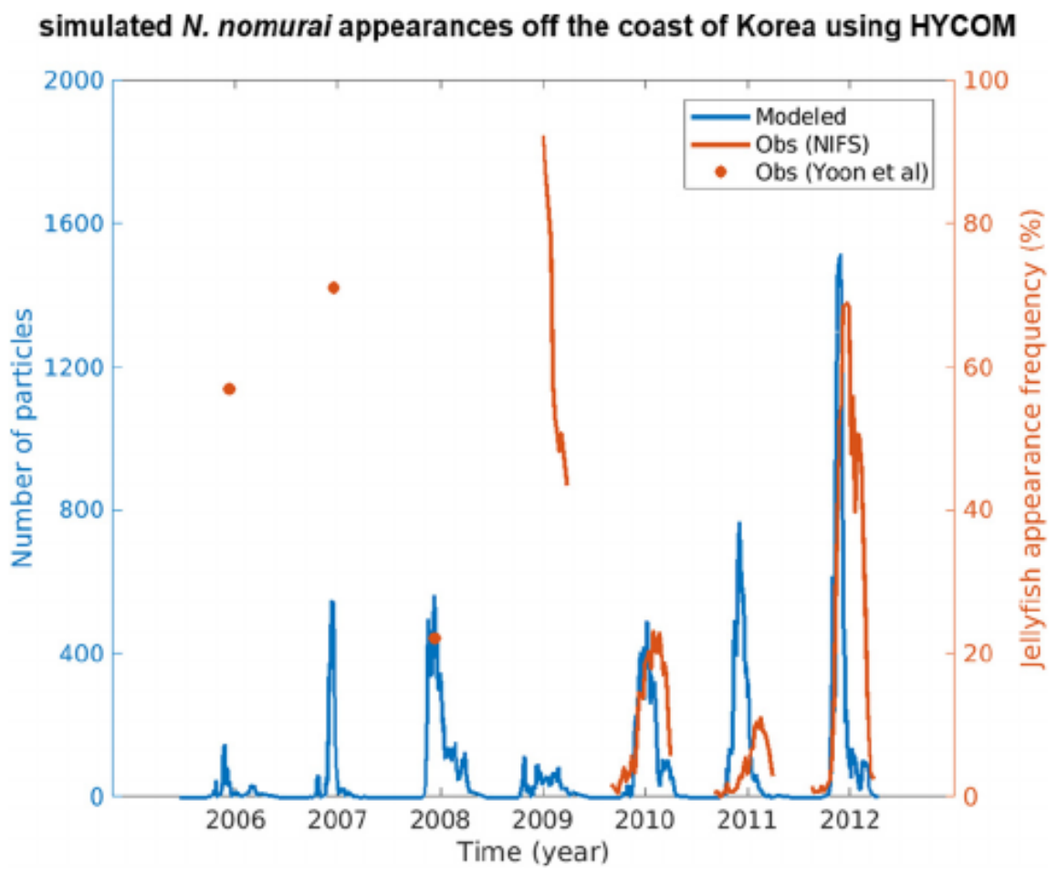

Fig. 10. Interannual *N. nomurai* appearances experiment results using HYCOM surface velocity field. Blue line is simulated time series for number of particles off the coast of Korea (Fig. 1, circles), and red line and dots are observed *N. nomurai* appearances off the coast of Korea from NIFS and Yoon et al. (2014), respectively. (For interpretation of the references to color in this figure legend, the reader is referred to the web version of this article.)

jellyfish appearance experiments are, in general, reasonably simulated (Fig. 9).

Velocity fields based on our simple model show better performance than the HYCOM reanalysis data for tracking jellyfish in the YS and ECS. HYCOM velocity fields indicate the presence of the Yellow Sea Warm Current that is inconsistent with observations. We presume that the presence of the Yellow Sea Warm Current at the surface caused significant differences between results using HYCOM velocity fields and those using the combined velocity fields proposed in this study. The poorer performance of the simulations using HYCOM relative to our data-derived velocity fields supports the conjecture that simple models can sometimes yield better results than a more complex model that is sensitive to uncertainties in many coefficients (Nof, 2008; Paudel and Jawitz, 2012; Orth et al., 2015). Velocity fields from numerical models are simulated by integrating initial and boundary conditions, and the uncertainties

data in the velocity fields. Nevertheless, it is a worth noting that the velocity fields simulate the outline of the location and distribution where observed jellyfish groups appear after approximately two months (Fig. 7a), and the results of the inter-annual

the YS and ECS (Moon et al., 2010; Son et al., 2015). In particular, Moon et al. (2010) focused on modeling a *N. nomurai* appearance event in the YS and ECS in 2005 using ROMS and denoted that wind was a key process governing *N. nomurai* distribution. The results of particle-tracking experiments in this study indicate that the wind determines not only the distribution of *N. nomurai* during a short-term event but also the number of *N. nomurai* reaching the coastal regions around the Korean Peninsula.

In the interannual simulation the particle distribution was primarily influenced by the East Asian Monsoon. When northerly winds from the winter Monsoon are sustained over the YS and ECS, southwestward Ekman currents prevented particles from moving toward the Korean Peninsula. On the contrary, southerly winds during the summer play a role in controlling the number of particles transported to the Korean Peninsula. Fig. 11 shows the mean velocity fields and accumulated distribution of particles during the summers of 2009 and 2014. Strong surface currents from the coast of China to the Korean Peninsula can be seen in 2009 (Fig. 11a) when the highest *N. nomurai* appearances were observed and a large number of particles were recorded. Conversely, in 2014, weak currents toward the Korean Peninsula occurred in the YS, resulting in relatively small number of particles arriving off the coast of Korea (Fig. 11b). This difference is attributed to seasonal variation in winds (see the wind rose in Fig. 11). Strong southerly winds during the summer occurred in 2009, and a weak easterly wind field was formed over the YS in 2014. This suggest that sufficiently strong southerly winds are associated with large jellyfish appearances off the coast of Korea, and that weak easterly wind fields in the YS (2014 and 2015) are associated with fewer jellyfish appearances.

To examine the influence of winds from each season, we calculated correlation coefficients between seasonal mean wind components and maximum *N. nomurai* appearances off the coast of the Korean Peninsula each year. The seasonal mean winds were calculated using the spatial mean and temporal three-month moving average. Zonal wind components did not show a significant relation, but meridional wind components showed relatively high correlation coefficients. In particular, winds before April had a strong relation with the *N. nomurai* appearances (correlation coefficient of 0.63). Winds after April had a weaker influence on *N. nomurai* appearances. April is when particles concentrated off the coast of China begin moving eastward. We presume that the Ekman currents off the coast of China until April can control the initial position of *N. nomurai* population before their eastward

in these conditions can propagate into the domain. The governing equations in chaotic numerical ocean modeling systems can be extremely sensitive to infinitesimal errors (Lorenz, 1963). On the other hand, the simple approach in this study directly estimates velocity fields from observed sea surface height derived from altimetry using the linear steady-state momentum equations. Although our model cannot resolve the full dynamics, it is directly based on observation and thus free from boundary and initial condition error propagation.

The results in this study imply that the simple method accounts for the dominant dynamics of jellyfish transport in the YS and ECS. In addition, the method has the advantage of computational efficiency and readily deducing the relative contributions of Ekman ($\vec{u}_e$) and geostrophic ($\vec{u}_g$) velocity components. Calculating the solution from Welander (1957) is significantly more efficient than solving the full primitive equation using more complex dynamical approaches. In general, the data method appears to be a useful tool for understanding the surface current systems of the YS and ECS.

4.2. Physical environment for N. nomurai transportation

Previous studies have shown that wind plays an important role in the transport of surface drifting objects, including jellyfish in

movement. Thus, the relation between winds before April and *N. nomurai* appearances off the Korean Peninsula can be influenced by different distributions of *N. nomurai* off the coast of China, which can be considered as an initial location for eastward transport of jellyfish.

To verify this supposition we conducted sensitivity tests of particle-tracking experiments using the climatological combined velocity fields from 2006 to 2015. Two groups of particles were launched off the Changjiang estuary in April. Each group comprised 10,000 particles and there was a 0.4° meridional distance between the two groups: A (black dot in Fig. 12a) and B (black dot in Fig. 12b). Fig. 12 shows that more particles from B border on the coast of Korea than particles from A. In addition, many particles from A are not transported to the YS and remained off the coast of China. The maximum number of particles off the coast of Korea from group A was 748, but for group B was 2176, approximately three times larger. This result implies that the surface currents off the coast of China determine the initial position of *N. nomurai* before they start moving eastward and the position affects the amount of *N. nomurai* transported toward the Korean Peninsula.

Interestingly, winds after April, when the *N. nomurai* are transported east, are qualitatively less correlated with jellyfish appearances at the Korean Peninsula. Even though the southerly wind

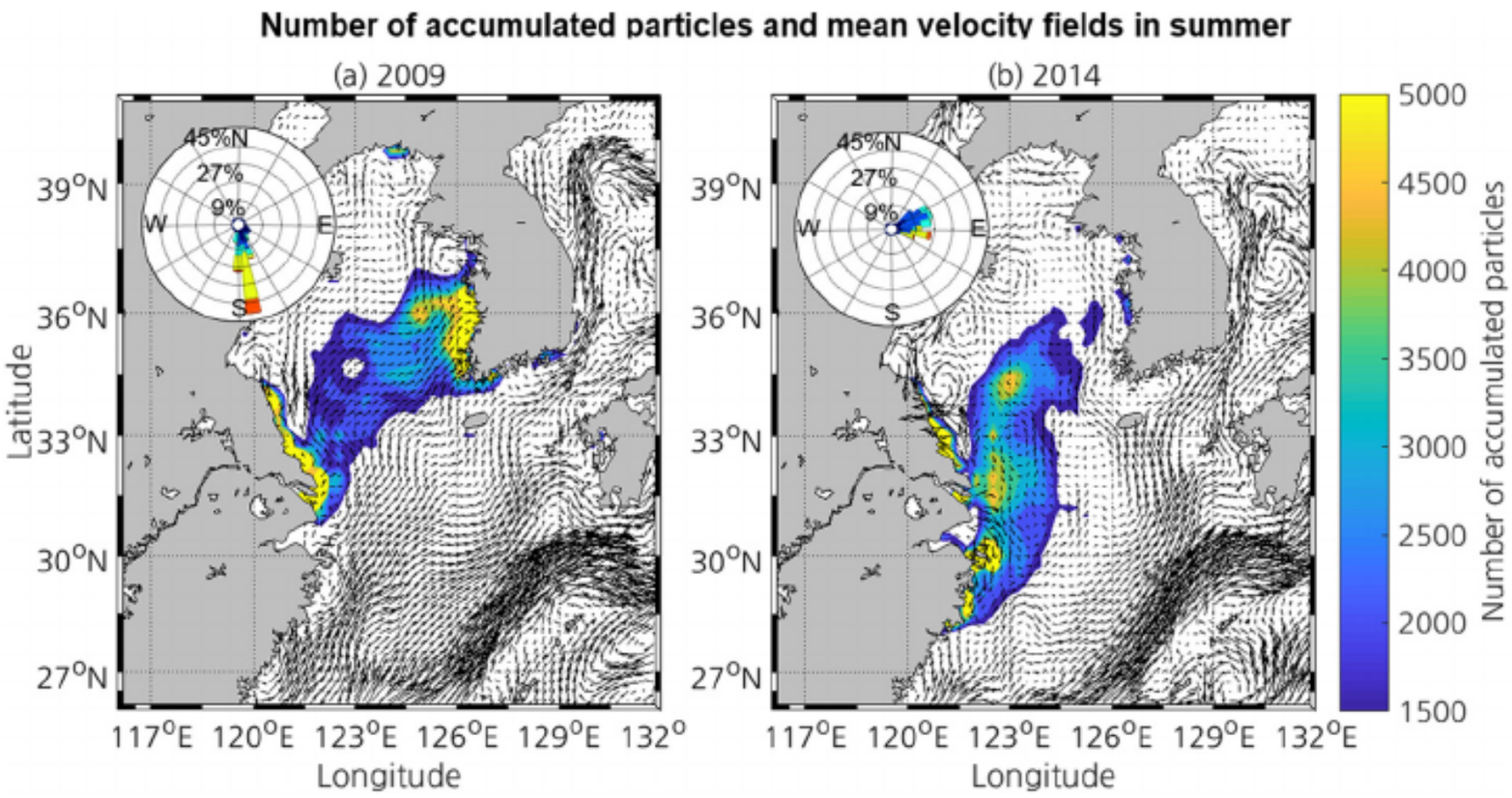

Fig. 11. Mean surface velocity field derived from the Ekman and geostrophic currents and the accumulated distribution of particles during the summers of 2009 (a) and 2014 (b). Color scale indicate accumulated number of particles during each summer.

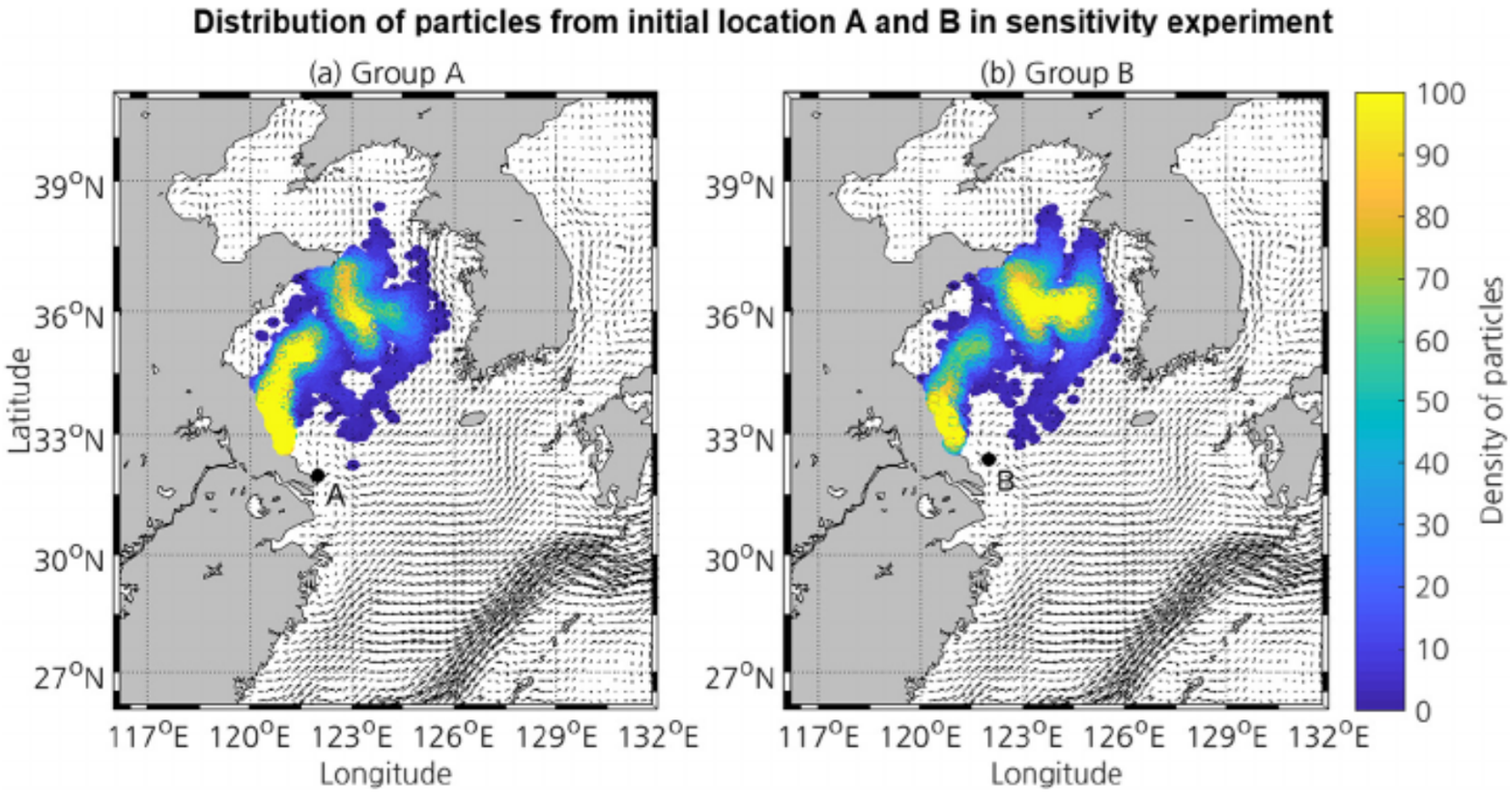

Fig. 12. Sensitivity of the particle-tracking experiment for relations between *N. nomurai* starting points off the east coast of China and appearance off the coast of Korea. (a) is the distribution of particles that are launched on the southern part and (b) is from the northern part. Each initial position is marked as a black dot. Color scale indicates particle density.

fields similar to those in 2009 frequently appeared in many other years (except for 2014 and 2015), the abundance of simulated particles and observed jellyfish off the coast of Korea varied in each year. This indicates that *N. nomurai* transport toward the Korean Peninsula is not caused by summer winds alone and can be affected by other velocity components, such as geostrophic currents. In winter, the magnitude of Ekman components is larger than geostrophic components in most of the YS (Fig. 4f). In summer, geostrophic components become more important, being as strong as Ekman components owing to weak wind stress (Fig. 4e). Accordingly, Ekman currents and geostrophic currents contribute similarly to summer surface current patterns. Consequently, oceanic forcing that can affect sea surface height, such as forcing from the Kuroshio Current, could also have an important role in the migration of *N. nomurai*. Fig. 13 shows that the population tracking experiment using each velocity component: geostrophic (Fig. 13a) and Ekman (Fig. 13b) velocities. When only one velocity component is considered, simulated particle distribution does not reproduce the observed jellyfish appearances (Fig. 3b). Between Jeju and Ieo Island, the simulations considering only geostrophic components better reproduced the observations than when considering only Ekman currents, suggesting that the geostrophic component could be more important than Ekman component.

In this work, we present a new approach to use data-derived velocity fields to simulate advection of surface drifting particles in the YS and ECS, and applied the method to simulate appearances of *N. nomurai* off the coast of Korea. Physical factors that can determine inter-annual appearances of *N. nomurai* around the Korean coast were identified. Recently, various biological disturbances such as green algae and sargassum masses have cropped up in the YS and ECS (Son et al., 2015; Komatsu et al., 2014). It is possible that our method can be extended to track these disturbances. In practice, when the combined velocity fields were applied to track green algae masses in 2011, which was reported and simulated by Son et al. (2015), the simulation using combined velocity shows rational results and the distribution of simulated particles (green dots in Fig. 14) agrees with observations (white squares in Fig. 14). Fig. 14 also shows the distribution of particles simulated by only one velocity component, either geostrophic currents (red dots in Fig. 14) or Ekman currents (blue dots in Fig. 14), neither of which alone reproduces the observations. This suggests that both velocity components should be considered concurrently to simulate advection of biological disturbances in the YS and ECS.

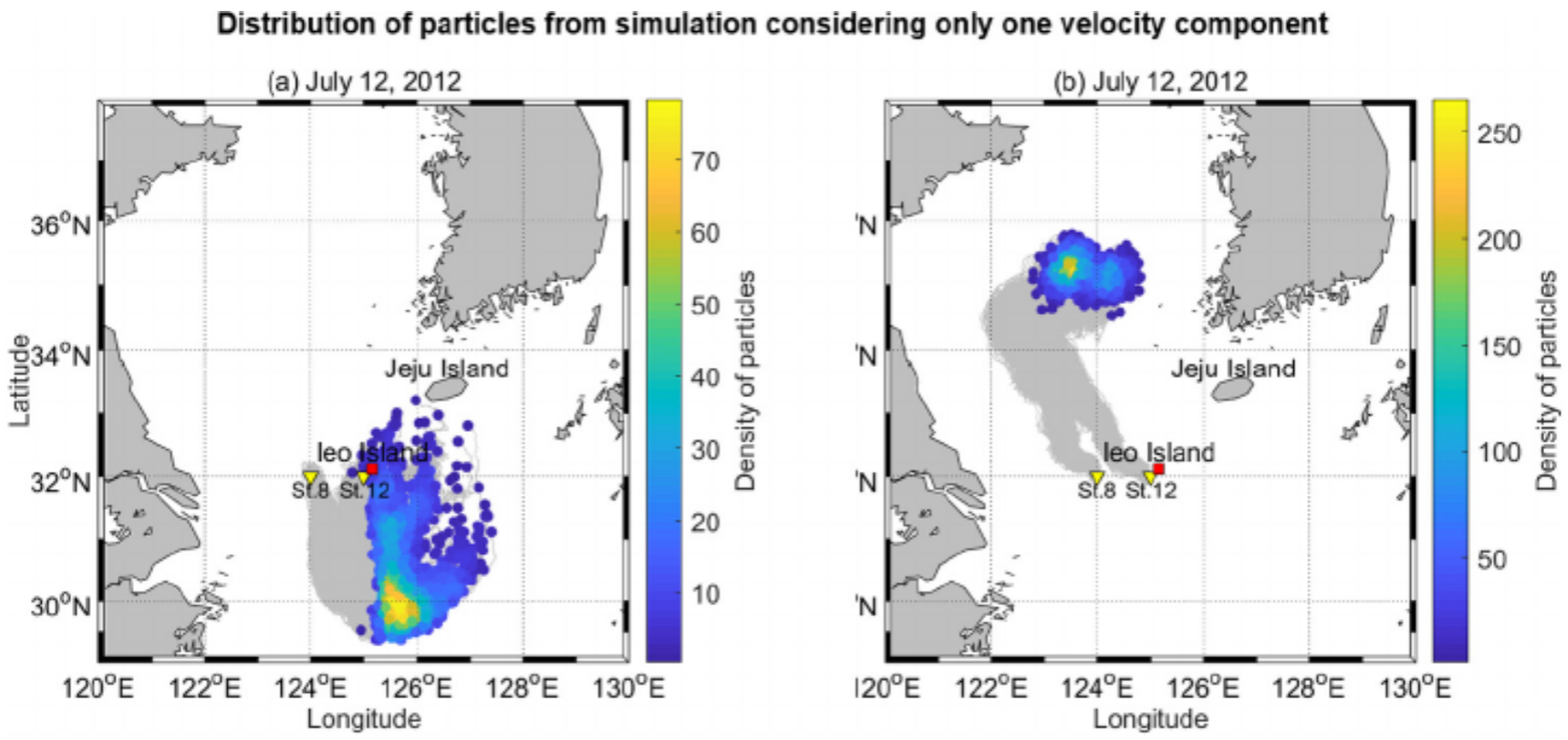

Fig. 13. Ideal population tracking experiments considering only each velocity component in the combined velocity fields: geostrophic (a) and Ekman (b) components. Color scales indicate particle density, and gray lines show trajectories of each particle.

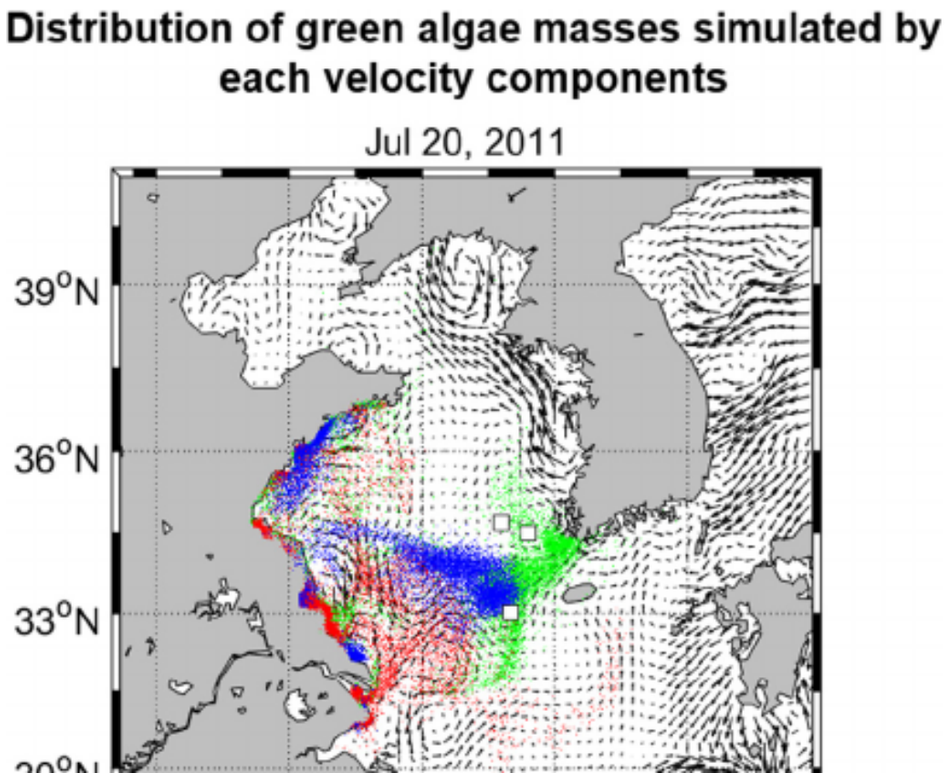

This research was supported by was a part of "Development of the Integrated Data Processing System for GOCI-II Research for Applications of Geostationary Ocean Color Imager" (Ministry of Oceans and Fisheries; 20150212) and was a part of the project titled 'Integrated management of marine environment and ecosystems around Saemangeum', funded by the Ministry of Oceans and Fisheries, Korea (grant number 20140257).

References

Ablain, M., Cazenave, A., Valladeau, G., Guinehut, S., 2009. A new assessment of the error budget of global mean sea level rate estimated by satellite altimetry over 1993–2008. Ocean Sci. 5, 193–201. http://dx.doi.org/10.5194/os-5-193-2009.

Amante, C., Eakins, B.W., 2009. ETOPO1 1 Arc-Minute Global Relief Model: Procedures, Data Sources and Analysis. NOAA Tech. Memo. NESDIS NGDC-24. http://dx.doi.org/10.1594/PANGAEA.769615.

Beardsley, R.C., Limeburner, R., Kim, K., Candela, J., 1992. Lagrangian flow observa-

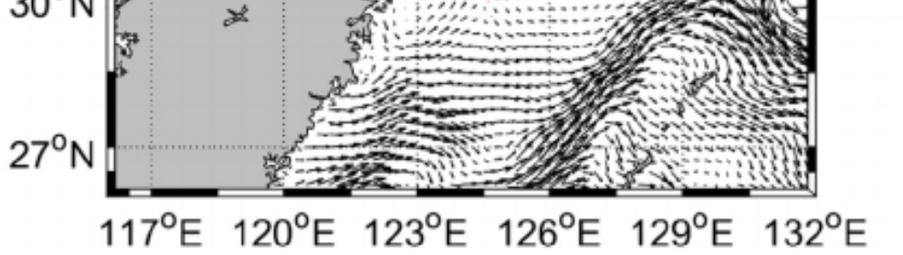

Fig. 14. Simulation results of green algae masses using components of the combined velocity fields. Distributions of particles are simulated by geostrophic components (red dots), Ekman components (blue dots), and combined velocity fields considering both component (green dots). Squares indicate locations where green algae masses were observed (Son et al., 2015). (For interpretation of the references to color in this figure legend, the reader is referred to the web version of this article.)

This simple approach is highly efficient and accessible. All simulations in this study can be conducted in a few hours using a personal computer, so the approach could be readily implemented by other researchers. Finally, the result that the combined velocity fields broadly simulates interannual changes in conservative particle transport (e.g., jellyfish advection), implies that interannual changes in surface current patterns in the YS and ECS is well reflected in the velocity fields, suggesting that this methodology may be useful to other research applications that consider interannual variability of current systems in the YS and ECS.

Acknowledgments

We gratefully acknowledge the editors and anonymous reviewers for their thoughtful comments that greatly improved the paper.

Kim, D.-H., Seo, J.-N., Yoon, W.-D., Suh, Y.-S., 2012. Estimating the economic damage caused by jellyfish to fisheries in Korea. Fish. Sci. 78, 1147–1152. http://dx.doi.org/10.1007/s12562-012-0533-1.

Komatsu, T., Mizuno, S., Natheer, A., Kantachumpoo, A., Tanaka, K., Morimoto, A., Hsiao, S.-T., Rothäusler, E., Shishidou, H., Aoki, M., Ajisaka, T., 2014. Unusual distribution of floating seaweeds in the East China Sea in the early spring of 2012. J. Appl. Phycol. 26, 1169–1179. http://dx.doi.org/10.1007/s10811-013-0152-y.

Lie, H., Cho, C.-H., Lee, J., Lee, S., 2001. Does the Yellow Sea Warm Current really exist as a persistent mean flow? 106, 22199–22210.

Lorenz, E.N., 1963. Deterministic nonperiodic flow. J. Atmos. Sci. 20, 130–141.

Mask, A.C., O'Brien, J.J., Preller, R., 1998. Wind-driven effects on the Yellow Sea Warm Current. J. Geophys. Res. Ocean. 103, 30713–30729. http://dx.doi.org/10.1029/1998JC900007.

Moon, J.-H., Pang, I.-C., Yang, J.-Y., Yoon, W.D., 2010. Behavior of the giant jellyfish Nemopilema nomurai in the East China Sea and East/Japan Sea during the summer of 2005: A numerical model approach using a particle-tracking experiment. J. Mar. Syst. 80, 101–114. http://dx.doi.org/10.1016/j.jmarsys.2009.10.015.

Naimie, C.E., Blain, C.A., Lynch, D.R., 2001. Seasonal mean circulation in the Yellow Sea - A model-generated climatology. Cont. Shelf Res. 21, 667–695. http://dx.doi.org/10.1016/S0278-4343(00)00102-3.

Nof, D., 2008. Simple versus complex climate modeling. Eos Trans. Am. Geophys. Union 89, 544–545.

Okuno, A., Watanabe, T., Honda, N., Takayama, K., 2011. Forecast of the giant jellyfish Nemopilema nomurai appearance in the Japan Sea, in: Oral Presentation at PICES 2011 Annual Meeting.

Orth, R., Staudinger, M., Seneviratne, S.I., Seibert, J., Zappa, M., 2015. Does model performance improve with complexity? A case study with three hydrological models. J. Hydrol. 523, 147–159. http://dx.doi.org/10.1016/j.jhydrol.2015.01.044.

Park, Y.-H., 1986. A simple theoretical model for the upwind flow in the southern yellow sea. J. Oceanol. Soc. Korea 21, 203–210.

Paudel, R., Jawitz, J.W., 2012. Does increased model complexity improve description of phosphorus dynamics in a large treatment wetland? Ecol. Eng. 42, 283–294. http://dx.doi.org/10.1016/j.ecoleng.2012.02.014.

Saraceno, M., Strub, P.T., Kosro, P.M., 2008. Estimates of sea surface height and near-surface alongshore coastal currents from combinations of altimeters and tide gauges. J. Geophys. Res. Ocean. 113, 1–20. http://dx.doi.org/10.1029/2008JC004756.

Seo, S., Park, Y., Park, J., Lee, H.J., Hirose, N., 2013. The tsushima warm current from a tion in the East China, Yellow and Japan Seas. La Mer 30, 297–314.

Bonjean, F., Lagerloef, G.S.E., 2002. Diagnostic model and analysis of the surface currents in the tropical pacific ocean. J. Phys. Oceanogr. 32, 2938–2954. http://dx.doi.org/10.1175/1520-0485(2002)032<2938:DMAAOT>2.0.CO;2.

Dee, D.P., Uppala, S.M., Simmons, A.J., Berrisford, P., Poli, P., Kobayashi, S., Andrae, U., Balmaseda, M.A., Balsamo, G., Bauer, P., Bechtold, P., Beljaars, A.C.M., van de Berg, L., Bidlot, J., Bormann, N., Delsol, C., Dragani, R., Fuentes, M., Geer, A.J., Haimberger, L., Healy, S.B., Hersbach, H., Hólm, E.V., Isaksen, L., Kållberg, P., Köhler, M., Matricardi, M., McNally, A.P., Monge-Sanz, B.M., Morcrette, J.-J., Park, B.-K., Peubey, C., de Rosnay, P., Tavolato, C., Thépaut, J.-N., Vitart, F., 2011. The ERA-Interim reanalysis: Configuration and performance of the data assimilation system. Q. J. R. Meteorol. Soc. 137, 553–597. http://dx.doi.org/10.1002/qj.828.

Ebisuzaki, W., 1997. A method to estimate the statistical significance of a correlation when the data are serially correlated. J. Clim. 10, 2147–2153.

Honda, N., Watanabe, T., Matsushita, Y., 2009. Swimming depths of the giant jellyfish Nemopilema nomurai investigated using pop-up archival transmitting tags and ultrasonic pingers. Fish. Sci. 75, 947–956. http://dx.doi.org/10.1007/s12562-009-0114-0.

Hong, J., Seo, S., Jeon, C., Park, J., Park, Y., Min, H.S., 2016. Evaluation of temperature and salinity fields of HYCOM reanalysis data in the east sea. Ocean Polar Res. 38, 271–286.

Hsueh, Y., Romea, R.D., Dewitt, P.W., 1986. Wintertime winds and coastal sea-level fluctuations in the northeast china sea. Part II: Numerical model. J. Phys. Oceanogr. 16, 241–261. http://dx.doi.org/10.1175/1520-0485(1986)016<0241:WWACSL>2.0.CO;2.

Ichikawa, H., Beardsley, R.C., 2002. The current system in the Yellow and East China Seas. J. Oceanogr. 58, 77–92. http://dx.doi.org/10.1023/A:1015876701363.

Johnson, E.S., Bonjean, F., Lagerloef, G.S.E., Gunn, J.T., Mrrchum, G.T., 2007. Validation and error analysis of OSCAR sea surface currents. J. Atmos. Ocean. Technol. 24, 688–701. http://dx.doi.org/10.1175/JTECH1971.1.

Kawahara, M., Uye, S.-I., Ohtsu, K., Iizumi, H., 2006. Unusual population explosion of the giant jellyfish Nemopilema nomurai (Scyphozoa: Rhizostomeae) in East Asian waters. Mar. Ecol. Prog. Ser. 307, 161–173. http://dx.doi.org/10.3354/meps307161.

Kim, C.-H., 1998. A Review of the yellow sea circulation models. Ocean Res. 20, 325–335.

Song, Y., Haidvogel, D., 1994. A semi-implicit ocean circulation model using a generalized topography-following coordinate system. J. Comput. Phys. http://dx.doi.org/10.1006/jcph.1994.1189.

Sun, S., Zhang, F., Li, C., Wang, S., Wang, M., Tao, Z., Wang, Y., Zhang, G., Sun, X., 2015. Breeding places, population dynamics, and distribution of the giant jellyfish Nemopilema nomurai (Scyphozoa: Rhizostomeae) in the Yellow Sea and the East China Sea. Hydrobiologia 59–74. http://dx.doi.org/10.1007/s10750-015-2266-5.

Tang, X., Wang, F., Chen, Y., Bai, H., Hu, D., 2004. Current observations in the southern Yellow Sea in summer. Chinese J. Oceanol. Limnol. 22, 217–223.

Teague, W.J., Jacobs, G.A., 2000. Current observations on the development of the Yellow sea warm current. J. Geophys. Res. 105, 3401–3411.

Toyokawa, M., Shibata, M., Cheng, J.-H., Li, H.-Y., Ling, J.-Z., Lin, N., Liu, Z.-L., Zhang, Y., Shimizu, M., Akiyama, H., 2012. First record of wild ephyrae of the giant jellyfish Nemopilema nomurai. Fish. Sci. 78, 1213–1218. http://dx.doi.org/10.1007/s12562-012-0550-0.

Uye, S., 2008. Blooms of the giant jellyfish Nemopilema nomurai: a threat to the fisheries sustainability of the East Asian Marginal Seas. Plankt. Benthos Res. 3, 125–131. http://dx.doi.org/10.3800/pbr.3.125.

Wei, H., Deng, L., Wang, Y., Zhao, L., Li, X., Zhang, F., 2015. Giant jellyfish Nemopilema nomurai gathering in the Yellow Sea—a numerical study. J. Mar. Syst. 144, 107–116. http://dx.doi.org/10.1016/j.jmarsys.2014.12.001.

Welander, P., 1957. Wind action on a shallow sea: some generalizations of Ekman's theory. Tellus 9, 45–52. http://dx.doi.org/10.3402/tellusa.v9i1.9070.

Willis, J., 2011. Modelling swimming aquatic animals in hydrodynamic models. Ecol. Modell. 222, 3869–3887. http://dx.doi.org/10.1016/j.ecolmodel.2011.10.004.

Yanagi, T., Morimoto, A., Ichikawa, K., 1997. Seasonal variation in surface circulation of the East China Sea and the Yellow Sea derived from satellite altimetric data. Cont. Shelf Res. 17, 655–664. http://dx.doi.org/10.1016/S0278-4343(96)00054-4.

Yoon, E.-A., Cha, C.-P., Hwang, D.-J., Yoon, Y.-H., Shin, H.-H., Gwak, D.-S., 2012. Interannual occurrence variation of the large jellyfish Nemopilema nomurai due to the changing marine environment in the East China Sea. J. Korean Soc. Fish. Technol. 48, 242–255. http://dx.doi.org/10.3796/KSFT.2012.48.3.242.

Yoon, W.D., Lee, H.E., Han, C., Chang, S.-J., Lee, K., 2014. Abundance and distribution of nemopilema nomurai (Scyphozoa, Rhizostomeae) in Korean Waters in 2005-2013. Ocean Sci. J. 49, 183–192. http://dx.doi.org/10.1007/s12601-014-0018-5.

Yoon, W.D., Yang, J.-Y., Shim, M.B., Kang, H.-K., 2008. Physical processes influencing the occurrence of the giant jellyfish Nemopilema nomurai (Scyphozoa: Rhizostomeae) around Jeju Island, Korea. J. Plankton Res. 30, 251–260. http://dx.doi.

high resolution ocean prediction model, HYCOM. Ocean Polar Res. 35, 135–146.
Sheng, J., Zhao, J., Zhai, L., 2009. Examination of circulation, dispersion, and connectivity in Lunenburg Bay of Nova Scotia using a nested-grid circulation model. J. Mar. Syst. 77, 350–365. http://dx.doi.org/10.1016/j.jmarsys.2008.01.013.
Son, Y.B., Choi, B., Kim, Y.H., Park, Y., 2015. Tracing floating green algae blooms in the Yellow Sea and the East China Sea using GOCI satellite data and Lagrangian transport simulations. Remote Sens. Environ. 156, 21–33. http://dx.doi.org/10.1016/j.rse.2014.09.024.
org/10.1093/plankt/fbm102.
Yu, F., Zhang, Z., Diao, X., Guo, J., 2010. Observational evidence of the Yellow Sea warm current. Chinese J. Oceanol. Limnol. 28, 677–683. http://dx.doi.org/10.1007/s00343-010-0006-2.
Zhang, Y., Liang, S., Sun, Z., 2017. Measurement and numerical study of vertical mixing microstructure in the bohai strait. J. Coast. Res. 33, 158–172. http://dx.doi.org/10.2112/JCOASTRES-D-15-00235.1.